nature geoscience

Article

https://doi.org/10.1038/s41561-023-01200-8

High natural nitric oxide emissions from lakes on Tibetan Plateau under rapid warming

Received: 20 August 2022

Accepted: 9 May 2023

Published online: 01 June 2023

Check for updates

Hao Kong[1], Jintai Lin[1] ✉, Yuhang Zhang[1], Chunjin Li[1], Chenghao Xu[1], Lu Shen[1], Xuejun Liu[2], Kun Yang[3,4], Hang Su[5,6] & Wanyun Xu[7]

Nitrogen oxides affect health and climate. Their emissions, in the form of nitric oxide, from inland waters such as lakes are generally considered negligible and are absent in air quality and climate models. Here we find unexpected high emissions of nitric oxide from remote lakes on the Tibetan Plateau, based on satellite observations of tropospheric nitrogen dioxide vertical column densities and subsequent emission inversion at a fine resolution of 5 km. The total emissions from 135 lakes larger than 50 km^2 reach 1.9 metric tons N h^{-1}, comparable to anthropogenic emissions in individual megacities worldwide or the Tibet Autonomous Region. On average, the emissions per unit area reach 63.4 μg N m^{-2} h^{-1}, exceeding those from crop fields. Such strong natural emissions from inland waters have not been reported, to the best of our knowledge. The emissions are derived from microbial processes in association with substantial warming and melting of glacier and permafrost on the plateau, constituting a previously unknown feedback between climate, lake ecology and nitrogen emissions.

Nitrogen oxides (NO_x = NO + NO_2) are important tropospheric constituents affecting human health, climate and ecosystems. NO_x are emitted mainly in the form of nitric oxide (NO), with the majority of NO quickly converted to nitrogen dioxide (NO_2) in the atmosphere through chemical reactions. Known major emission sources of NO include combustion, lightning and microbial processes. In water, NO is produced by nitrite photolysis[1] and microbial activities[2,3], often together with production of nitrous oxide (N_2O) (refs. 2,3). Emissions of NO from water into the atmosphere are generally thought to be trivial, especially in remote regions with few local human influences such as the Tibetan Plateau (TP). Yet, here we show unexpected high NO emissions from the TP lakes, which are potentially linked to amplified warming over the TP[4,5] and its unique ecological environment, based on satellite retrieval of tropospheric NO_2 vertical column densities (VCDs) and subsequent emission estimate.

NO emissions from water have traditionally been considered unimportant for several reasons. Although nitrite photolysis can lead to generation of NO in surface seawater[1], the generated NO can be quickly consumed before being emitted into the atmosphere[1]. Microbial activities can also result in NO emissions through the nitrification–denitrification processes. However, laboratory studies[6] and in situ measurements[1,7,8] have shown N_2O to be a much more important water-sourced product than NO. The anaerobic ammonium oxidation (that is, anammox) process is another important microbial pathway for nitrogen loss in water under anaerobic conditions, as has been widely exploited in wastewater treatment[6,9]. The anammox process can lead to emissions of NO but not N_2O, since N_2O-forming genes are

[1]Laboratory for Climate and Ocean-Atmosphere Studies, Department of Atmospheric and Oceanic Sciences, School of Physics, Peking University, Beijing, China. [2]College of Resources and Environmental Sciences, National Academy of Agriculture Green Development, China Agricultural University, Beijing, China. [3]Ministry of Education Key Laboratory for Earth System Modeling, Department of Earth System Science, Tsinghua University, Beijing, China. [4]National Tibetan Plateau Data Center, State Key Laboratory of Tibetan Plateau Earth System and Resource Environment, Institute of Tibetan Plateau Research, Chinese Academy of Sciences, Beijing, China. [5]Multiphase Chemistry Department, Max Planck Institute for Chemistry, Mainz, Germany. [6]Institute of Atmospheric Physics, Chinese Academy of Sciences, Beijing, China. [7]State Key Laboratory of Severe Weather & Key Laboratory for Atmospheric Chemistry of CMA, Institute of Atmospheric Composition, Chinese Academy of Meteorological Sciences, Beijing, China. ✉e-mail: linjt@pku.edu.cn

https://doi.org/10.1038/s41561-023-01200-8

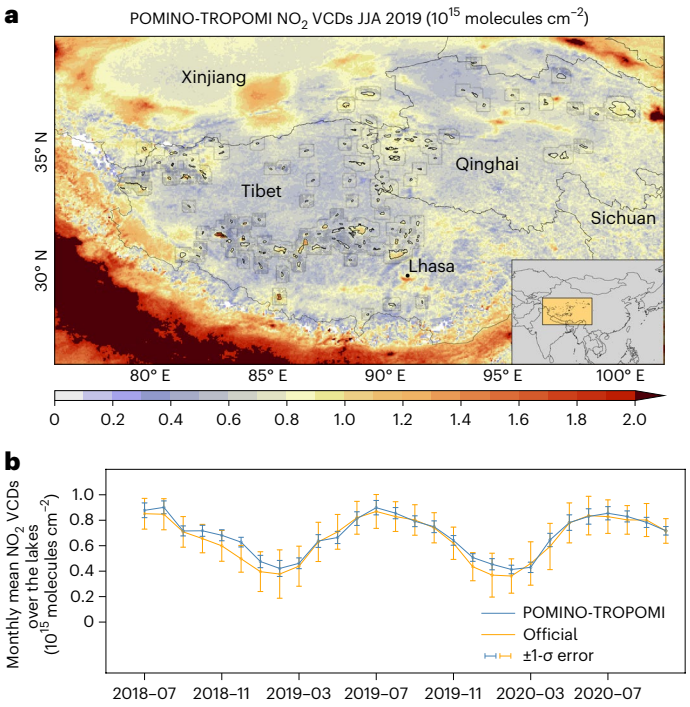

Fig. 1 | High NO_2 signals over TP lakes. a, POMINO-TROPOMI NO_2 VCDs at 0.05° × 0.05° over the TP. The 135 lakes selected in our study are outlined with black lines, with the area within a distance of 20 km of each lake outlined with thinner lines. The high mountains within 20 km of each lake with the mountain–lake elevation difference exceeding 500 m are shown in shadow. Sichuan, Qinghai, Xinjiang, Tibet and Lhasa City are depicted. The location of TP in Asia is shown in the inlet. **b**, Monthly mean NO_2 VCDs over the 135 lakes from July 2018 to October 2020 based on POMINO-TROPOMI[20] and the official product[35]. The error bars (±1-σ, one standard error) denote the average error among the 2,116 grid cells covering the 135 lakes; the VCD error of each grid cell is estimated following ref. 21. The elevation data are from the GLOBE project[36] (last access 26 May 2020). The location and shape data of lakes are from the HydroLAKES database[37] (last access 1 December 2021).

absent from such bacteria[3]. Yet, the role of anammox in NO emissions from inland waters remains little known. So far, most studies of nitrogen emissions from water are focused on N_2O (ref. 10); and NO emissions from water are not represented in air quality models and Earth system models[11,12].

The TP is known as the 'Third Pole' and 'Asian Water Tower' supplying water resources for almost 2 billion people. It contains thousands of lakes that together contribute more than half of the total lake area in China[13]. Most of the TP lakes are located in remote regions away from human activities and are very sensitive to climate change[13,14]. Most TP lakes are closed[15] with no water outflow, and the lake water environments are basically alkaline[15] and saline[10,15]. Due to amplified warming (about 0.40 °C dec^{-1} in summer)[4] and melting of permafrost and glaciers[16,17] on the TP, the number and volume of its lakes are growing[18,19] and the ice-free periods of large lakes are getting longer. In situ flux measurements of N_2O and other greenhouse gases from the TP lakes[10] have suggested potential positive feedbacks between greenhouse gas emissions and climate warming. However, in situ measurements of NO emissions from the TP lakes have been excluded in part because of the traditional view that such emissions are negligible[6].

In this Article, we quantify summertime NO emissions from the TP lakes at a high resolution of 0.05° × 0.05° (approximately 5 km × 5 km), by employing the POMINO-TROPOMI satellite product[20] for tropospheric NO_2 VCDs and the PHLET algorithm[21] for emission inversion, as detailed in Methods. Our results reveal high NO emissions over the TP lakes from microbial processes under rapid warming.

Strong signal of NO_2 VCDs over lakes

Figure 1a shows the POMINO-TROPOMI NO_2 VCD data in summer (June, July and August) 2019 over the TP on a 0.05° × 0.05° grid. The NO_2 VCDs are relatively low in most areas due to small anthropogenic influences. However, NO_2 hotspots exist over a few cities (for example, Lhasa, the Capital City of Tibet) and many lakes. The lakes on the southern TP show the most notable NO_2 hotspots. The highest value over the Nangla Ringco lake reaches 4.1×10^{15} molecules cm^{-2}, comparable to those over the polluted regions in eastern China[21].

Considering the horizontal resolution of satellite data, our analysis is focused on the lakes with area larger than 50 km^2. To select the lakes away from human influences, we remove those within a distance of 20 km of which the average nighttime light brightness[22] exceeds 3 bits and/or the average population density[23] exceeds 10 km^{-2}. In total, we select 135 lakes that together occupy more than 60% of the total lake area on the TP. About 66% of these selected lakes are located between 4.5 km and 5.0 km above sea level, where the severest degradation of glaciers and permafrost occurs[24]. The population density within 20 km of a lake is lower than 1.5 km^{-2} for 84% of these lakes.

Each of the 135 lakes occupies multiple grid cells. The average NO_2 VCD over each lake varies from 0.49×10^{15} to 1.43×10^{15} molecules cm^{-2} with a 135-lake average of 0.81×10^{15} molecules cm^{-2}. The NO_2 levels over the lakes tend to be higher than over their surroundings within a distance of 20 km, especially for those over the southern TP—their NO_2 values exceed the surroundings by 31.2% on average, with the difference larger than the relative error of satellite data (about 20% in low-aerosol situations[20]). The NO_2 contrast is particularly evident along the geographical boundaries of several large lakes (Fig. 1a). To test the statistical significance of the NO_2 differences between the 135 lakes and their surroundings, we apply two-sample two-tailed t-test to each lake on the basis of NO_2 data at individual grid cells. There are 120 lakes (89%) with higher mean NO_2 VCDs than their surroundings; and for 111 lakes, NO_2 VCDs over lakes exceed their surroundings with P value less than 0.01 (Supplementary Data).

To further evaluate the lake NO_2 signals, Supplementary Data shows the spatial peak signal-to-noise ratio (PSNR) for each lake:

$$\mathrm{PSNR} = \frac{\max(\mathrm{VCD_{lake}}) - \mathrm{mean}(\mathrm{VCD_{sur}})}{\mathrm{std}(\mathrm{VCD_{sur}})}$$

Here VCD_{lake} stands for NO_2 VCDs at the 0.05° × 0.05° grid cells covering a given lake; and VCD_{sur} stands for NO_2 at the non-lake grid cells within 20 km of that lake. On average among the 135 lakes, the standard deviation of NO_2 VCDs for the surroundings ($std(VCD_{sur})$) is about 28% of $mean(VCD_{sur})$, which is larger than the relative error of retrieved VCDs (about 20%) (ref. 20). Among the 120 lakes with $mean(VCD_{lake}) > mean(VCD_{sur})$, 95% show PSNR values larger than 1.

Our additional tests suggest that the high NO_2 signals over the lakes are not caused by satellite retrieval errors associated with surface reflectance. We scale surface reflectance over the lakes by half or two times, and follow the POMINO-TROPOMI retrieval process to re-derive the NO_2 VCDs for July 2019. As detailed in Extended Data Fig. 1, changing the surface reflectance does not lead to substantial changes in NO_2 VCDs over the lakes. Also, no major changes are found in PSNR (Supplementary Data). The lake NO_2 signals are also not a result of satellite retrieval errors associated with clouds, aerosols and a priori NO_2 vertical profiles, as discussed in Methods. Thus, the robustness of the relative difference between the lakes and their surroundings is not sensitive to the NO_2 retrieval error.

We further examine the seasonality of NO2 VCDs over the 135 lakes (Fig. 1b) from July 2018 to October 2020 to explore their sources. It

exhibits a strong seasonal cycle, with the summer peak value about twice the winter minimum. Similar seasonality is shown in the official NO_2 product by KNMI. The seasonal cycle suggests natural, microbial sources[25] that peak in summer. On the contrary, anthropogenic sources would have led to the opposite summer–winter NO_2 contrast due to a much longer lifetime and higher emissions (for example, from heating) in winter.

Substantial NO emissions from lakes

Figure 2a shows NO emissions over the 135 lakes and their surroundings derived on the basis of a modified version of our PHLET algorithm (Methods). More detailed information for emissions and uncertainties is presented in Supplementary Data for all lakes and in Fig. 2b for the top ten emitting lakes. Emission uncertainties are caused by errors in satellite data and emission inversion[21], and are expressed as one standard deviation here. Of the 135 lakes, the highest emission on a per unit area basis occurs over Ngangla Ringco with a value as high as 174.1 ± 19.0 μg N m^{-2} h^{-1}. The emission per unit area exceeds 100 μg N m^{-2} h^{-1} for 12 lakes and exceeds 50 μg N m^{-2} h^{-1} for 52 lakes. Averaged over all lakes, the emission per unit area is about 63.4 μg N m^{-2} h^{-1}. These values are higher than annual averages from Chinese crop fields (6.5–21 μg N m^{-2} h^{-1}) (ref. 26).

Together, the 135 lakes emit NO at a level of 1.89 ± 0.54 metric tons N h^{-1}, which are more than three times of anthropogenic emissions (0.60 ± 0.17 tons N h^{-1}) in Lhasa[21] and are similar to anthropogenic emissions of Tibet Autonomous Region in the inventories (MEIC: 1.85 tons N h^{-1} in summer 2017; PKU-NO_x: 1.71 tons N h^{-1} in summer 2014) (refs. 27,28). The total lake emissions are comparable to anthropogenic emissions in the megacities worldwide, such as Beijing (7.8 tons N h^{-1}) (ref. 21), New York City (3.0 tons N h^{-1}) (ref. 29), Paris (0.3 tons N h^{-1}) (ref. 29) and London (1.7 tons N h^{-1}) (ref. 29).

Five of the top ten emitting lakes are located to the north of the Gangdisi Range (GR) and between the Tangula Range (TR) and the Nyainqentanglha Range (NR) (Fig. 2a). The other five lakes are in the birth regions of the Indus River (IR), the Yangtze River (YZR) and the Yellow River (YR), or close to the Kunlun Range (KR) and the Arkin Range (AR). The locations of these ten lakes match those experiencing growth in area over the past decades[30] associated with rapid warming over the TP[4]. The emission from Qinghai Lake alone (0.24 ± 0.027 tons N h^{-1}) is equivalent to that from a coal-fired power plant with capacity of 400–450 MW (ref. 31).

We compare the NO emissions with available in-situ measurements of N_2O fluxes for 11 lakes in 2014 and 2015 from May to August[10]. The NO emissions are about 10 times of N_2O averaged over the 11 lakes (Supplementary Data). The NO emissions in Ta-tse (denoted as Dogze Co in ref. 10; matched by location) are more than 70 times the N_2O emissions. These results are in contrast to previous studies suggesting much larger emissions of N_2O than NO over the oceans, inland waters and wetlands[1,7,8].

The high NO emissions from these TP lakes are linked to the unique, rapidly changing environment on the plateau affecting lake microbial activities. The TP is experiencing rapid warming[4], melting of permafrost and glaciers, growth in lake number and volume, and enhancement in nitrogen nutrition delivery into the lake water[32]. Most TP lakes are closed, saline and alkaline, and their surface waters contain low concentrations of chlorophyll-a and fluorescent dissolved organic matter[15]. Both nitrification–denitrification bacteria and anammox bacteria exist in these lakes[33]. Meanwhile, the emitted NO from the TP lakes will further affect the climate and ecosystems. For example, the lake-emitted NO may lead to effective production of ozone, which in turn enhances warming. The lake NO emissions may also enhance nitrogen deposition to the regional ecosystems. In fact, increasing deposition of oxidized nitrogen has been observed in several regions of the TP[34]. This suggests important feedbacks between climate change, lake ecology and nitrogen emissions not recognized before.

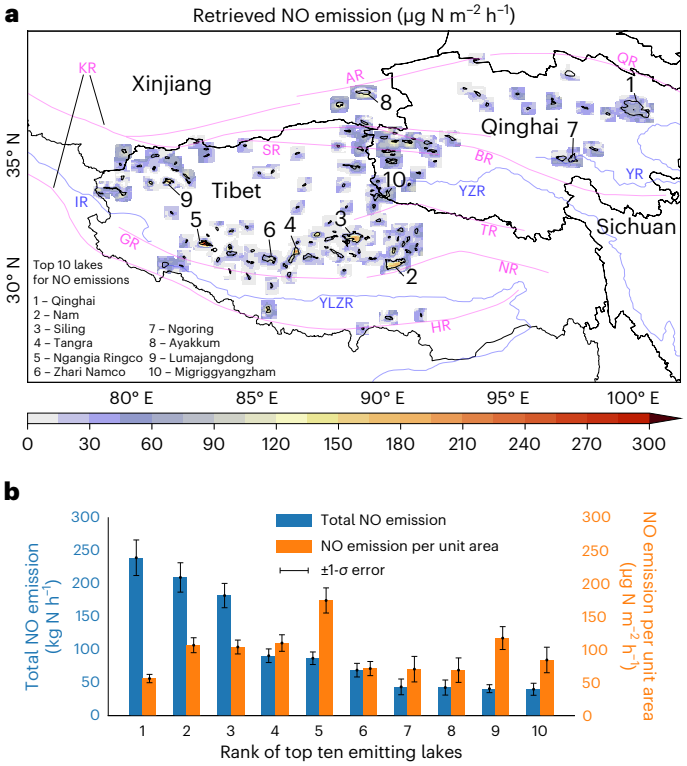

Fig. 2 | Substantial NO emissions from TP lakes. a, Retrieved NO emissions at 0.05° × 0.05°. The purple lines depict the locations of main mountain ranges, and the blue lines depict the locations of major rivers. The top ten emitting lakes are also depicted. **b**, Total NO emissions and NO emissions per unit area of the top ten emitting lakes. Data are presented as mean values ± one standard deviation. Data for all 135 lakes are detailed in Supplementary Data. Error bars are ±1-σ (one standard error).

Given the high emissions of NO from the TP lakes revealed from space, we call for in situ measurements of NO fluxes and laboratory experiments to obtain further evidence of such emissions and their exact microbial mechanisms and processes. Inclusion of such emission processes in the models is needed to investigate the potential feedback of lake NO emissions to the climate system. The high NO emissions might also occur over other lakes and inland waters worldwide, through similar or different microbial mechanisms. Future investigation will be important for understanding the ecological and environmental changes over these little-known, vital regions under rapid climate change. Further, our study also points to the value of high-resolution satellite remote sensing and emission inversion method in quantitatively detecting environmental changes over remote regions to provide a full picture of how the Earth environment evolves under human influence and natural variability.

Online content

Any methods, additional references, Nature Portfolio reporting summaries, source data, extended data, supplementary information, acknowledgements, peer review information; details of author contributions and competing interests; and statements of data and code availability are available at https://doi.org/10.1038/s41561-023-01200-8.

References

1. Tian, Y. et al. Nitric oxide (NO) in the Bohai Sea and the Yellow Sea. *Biogeosciences* **16**, 4485–4496 (2019).

2. Klotz, M. G. *Research on Nitrification and Related Processes, Part 1* (Academic Press, 2011).
3. Klotz, M. G. *Research on Nitrification and Related Processes, Part 2* (Academic Press, 2011).
4. Peng, X. et al. Assessment of temperature changes on the Tibetan Plateau during 1980–2018. *Earth Space Sci.* **8**, e2020EA001609 (2021).
5. Chen, D. et al. Assessment of past, present and future environmental changes on the Tibetan Plateau. *Chin. Sci. Bull.* **60**, 3025–3035 (2015).
6. Kampschreur, M. J. et al. Emission of nitrous oxide and nitric oxide from a full-scale single-stage nitritation-anammox reactor. *Water Sci. Technol.* **60**, 3211–3217 (2009).
7. Deng, J. et al. Annual emissions of nitrous oxide and nitric oxide from rice-wheat rotation and vegetable fields: a case study in the Tai-Lake region, China. *Plant Soil* **360**, 37–53 (2012).
8. Arévalo-Martínez, D. L., Kock, A., Löscher, C. R., Schmitz, R. A. & Bange, H. W. Massive nitrous oxide emissions from the tropical South Pacific Ocean. *Nat. Geosci.* **8**, 530–533 (2015).
9. Kuenen, J. G. Anammox bacteria: from discovery to application. *Nat. Rev. Microbiol.* **6**, 320–326 (2008).
10. Yan, F. et al. Lakes on the Tibetan Plateau as conduits of greenhouse gases to the atmosphere. *J. Geophys. Res.* **123**, 2091–2103 (2018).
11. Dunne, J. P. et al. The GFDL Earth System Model Version 4.1 (GFDL-ESM 4.1): overall coupled model description and simulation characteristics. *J. Adv. Model. Earth Syst.* **12**, e2019MS002015 (2020).
12. Guenther, A. B. et al. The model of emissions of gases and aerosols from Nature version 2.1 (MEGAN2.1): an extended and updated framework for modeling biogenic emissions. *Geosci. Model Dev.* **5**, 1471–1492 (2012).
13. Dou, X. et al. Spatio-temporal evolution of glacial lakes in the Tibetan Plateau over the past 30 years. *Remote Sens.* **15**, 416 (2023).
14. Lei, Y. et al. Response of inland lake dynamics over the Tibetan Plateau to climate change. *Clim. Change* **125**, 281–290 (2014).
15. Liu, C. et al. In-situ water quality investigation of the lakes on the Tibetan Plateau. *Sci. Bull.* **66**, 1727–1730 (2021).
16. Cheng, G. et al. Characteristic, changes and impacts of permafrost on Qinghai-Tibet Plateau. *Chin. Sci. Bull.* **64**, 2783–2795 (2019).
17. Yao, T. et al. Different glacier status with atmospheric circulations in Tibetan Plateau and surroundings. *Nat. Clim. Change* **2**, 663–667 (2012).
18. Zhang, G. et al. Lake volume and groundwater storage variations in Tibetan Plateau's endorheic basin. *Geophys. Res. Lett.* **44**, 5550–5560 (2017).
19. Zhou, J. et al. Quantifying the major drivers for the expanding lakes in the interior Tibetan Plateau. *Sci. Bull.* **67**, 474–478 (2021).
20. Liu, M. et al. A new TROPOMI product for tropospheric NO_2 columns over East Asia with explicit aerosol corrections. *Atmos. Meas. Tech.* **13**, 4247–4259 (2020).
21. Kong, H. et al. Considerable unaccounted local sources of NO_x emissions in China revealed from satellite. *Environ. Sci. Technol.* **56**, 7131–7142 (2022).
22. Li, X. & Zhou, Y. A stepwise calibration of global DMSP/OLS stable nighttime light data (1992–2013). *Remote Sens.* **9**, 637 (2017).
23. Center for International Earth Science Information Network - CIESIN - Columbia University. *Gridded Population of the World, Version 4 (GPWv4): Population Count* (NASA Socioeconomic Data and Applications Center, 2016).
24. Zhang, Y., Yan, J., Cheng, X. & He, X. Wetland changes and their relation to climate change in the Pumqu Basin, Tibetan Plateau. *Int. J. Environ. Res. Public Health* **18**, 2682 (2021).
25. Weng, H. et al. Global high-resolution emissions of soil NO_x, sea salt aerosols, and biogenic volatile organic compounds. *Sci. Data* **7**, 148 (2020).
26. Yao, Z. et al. Reducing N_2O and NO emissions while sustaining crop productivity in a Chinese vegetable–cereal double cropping system. *Environ. Pollut.* **231**, 929–941 (2017).
27. Zheng, B. et al. Trends in China's anthropogenic emissions since 2010 as the consequence of clean air actions. *Atmos. Chem. Phys.* **15**, 14095–14111 (2018).
28. Huang, T. et al. Spatial and temporal trends in global emissions of nitrogen oxides from 1960 to 2014. *Environ. Sci. Technol.* **51**, 7992–8000 (2017).
29. Crippa, M. et al. High resolution temporal profiles in the Emissions Database for Global Atmospheric Research. *Sci. Data* **7**, 121 (2020).
30. Zhang, G. et al. 100 years of lake evolution over the Qinghai–Tibet Plateau. *Earth Syst. Sci. Data* **13**, 3951–3966 (2021).
31. Liu, X. et al. Updated hourly emissions factors for Chinese power plants showing the impact of widespread ultralow emissions technology deployment. *Environ. Sci. Technol.* **53**, 2570–2578 (2019).
32. Su, Y. et al. Effects of climate change and nutrient concentrations on carbon sources for zooplankton in a Tibetan Plateau lake over the past millennium. *J. Paleolimnol.* **68**, 249–263 (2022).
33. Mukan, J. I. *Bacteria Distribution in Tibetan lakes (Version 1.0) (2015)* (A Big Earth Data Platform for Three Poles, 2018).
34. Wang, W. et al. Characteristics of atmospheric reactive nitrogen deposition in Nyingchi City. *Sci. Rep.* **9**, 4645 (2019).
35. Geffen, J. H. G. M. v., Eskes, H. J., Boersma, K. F. & Veefkind, J. P. TROPOMI ATBD of the total and tropospheric NO_2 data products. **2.4.0**, 1–88 (2021).
36. Hastings, D. A. & Dunbar, P. K. *Global Land One-Kilometer Base Elevation* (GLOBE, 1993).
37. Messager, M. L., Lehner, B., Grill, G., Nedeva, I. & Schmitt, O. Estimating the volume and age of water stored in global lakes using a geo-statistical approach. *Nat. Commun.* **7**, 13603 (2016).

Methods

Satellite NO_2 VCDs

The TROPOMI sensor offers unprecedented high-resolution monitoring of NO_2 with a pixel size of 3.5 km × 5.5 km at nadir view. The POMINO-TROPOMI product of tropospheric NO_2 VCDs (ref. 20) is an improved regional research product upon the official product by KNMI[35]. POMINO-TROPOMI covers most of East Asia, South Asia and Southeast Asia. The POMINO algorithm re-calculates air mass factors to convert tropospheric slant column densities (taken from the official product) to VCDs[20,38,39], with the consideration that the air mass factor calculation is the dominant error source for tropospheric NO_2 retrieval. Compared with the official product, the POMINO-TROPOMI algorithm explicitly accounts for the effects of aerosols and surface reflectance anisotropy, and uses a priori NO_2 vertical profile data at a higher horizontal resolution (25 km versus 100 km) (refs. 20,38–40). Thus, it reduces the bias against ground-based MAX-DOAS measurements and has more valid data points especially in heavy pollution situations[20,21]. The POMINO products have been widely used to study air pollution, NO emissions and nitrogen deposition[21,41]. We adopt the Level-2 POMINO-TROPOMI NO_2 data for June, July and August 2019 and map them on a 0.05° × 0.05° grid.

We conducted additional tests to investigate the extent to which the high NO_2 VCD signals from the TP lakes can be affected by potential errors in the satellite retrieval process. Major factors affecting the NO_2 retrieval include prerequisite cloud retrieval, aerosols, a priori profiles of NO_2 and surface reflectance[38]. Following common practice, we have filtered out the satellite pixels with cloud radiance fraction (CRF) larger than 0.5 to reduce cloud contamination. The distribution of CRF from valid pixels shows no systemic differences between the lakes and their nearby regions (Extended Data Fig. 2), suggesting that potential errors in clouds, if any, should not have led to the lake-specific high NO_2 VCD signals. Aerosol loadings are generally small over the TP lakes (see aerosol optical depth in Extended Data Fig. 3)[20,42], and thus should not affect the NO_2 retrieval over these areas substantially. The a priori profiles of NO_2 are adopted from GEOS-Chem simulations[40], for which we find no reasons to lead to arbitrary, lake-specific high NO_2 signals. To test the effect of surface reflectance on NO_2 retrieval, we halve or double the surface reflectance over the lakes and find no substantial impacts on the retrieved NO_2 VCDs.

NO emission inversion

To estimate NO emissions from the lakes, we adopt our PHLET-based emission inversion algorithm[21]. PHLET is a two-dimensional (longitude and latitude) model describing the relation between NO emissions and NO_2 VCDs averaged over a period (June, July, August 2019 here). It accounts for non-linear chemistry, temporal average advection and 'effective' diffusion of NO_2 due to deviation of winds from their temporal average. Together with its adjoint, the PHLET model offers efficient, robust inversion of NO emissions from NO_2 VCDs at a high resolution (0.05° × 0.05°). By default, PHLET uses wind fields in the lower troposphere (0–500 m above the ground, where surface-sourced NO_x is concentrated) to simulate horizontal transport of NO_2. The wind data are taken from the assimilated meteorological dataset GEOS-FP[43] at a horizontal resolution of 0.3125° longitude × 0.25° latitude and a temporal resolution of 3 h. Emission errors caused by uncertainties in the satellite NO_2 data and in the individual steps of emission inversion are discussed step by step in our previous work[21].

We further modify the emission retrieval algorithm to accommodate the special topography surrounding the TP lakes. These lakes are often located in valleys surrounded by mountains, where the elevation drops typically exceed 500 m (Fig. 1a) within a small horizontal distance (<20 km), according to the GLOBE Elevation Data[36]. Thus, horizontal transport of near-surface NO_2 is rather small. However, the available wind data do not have a sufficiently high resolution to represent the effect of such large elevation gradient on local atmospheric circulation. Using the 0–500 m average winds as default would overestimate the horizontal transport of near-surface NO_2 and lead to mis-location of emission sources. Thus, we use wind data in the bottom layer of GEOS-FP (about 0–120 m above the ground). We further exclude the temporal average advection and consider only the 'effective' horizontal diffusion of NO_2. In addition, we assign extremely large uncertainties (1.0×10^{99} molecules cm^{-2}) to NO_2 VCDs over the high mountains within 20 km of each lake where the mountain–lake elevation difference exceeds 500 m (Fig. 1a).

Data availability

NO_2 VCD and NO emission data produced in this study are available in Supplementary Data. Data obtained from publicly available sources are available from the references. Source data are provided with this paper.

Code availability

Codes for NO_2 VCD retrieval and NO emission inversion are available on a collaboration basis.

References

38. Lin, J. T. et al. Retrieving tropospheric nitrogen dioxide from the Ozone Monitoring Instrument: effects of aerosols, surface reflectance anisotropy, and vertical profile of nitrogen dioxide. *Atmos. Chem. Phys.* **14**, 1441–1461 (2014).
39. Liu, M. et al. Improved aerosol correction for OMI tropospheric NO_2 retrieval over East Asia: constraint from CALIOP aerosol vertical profile. *Atmos. Meas. Tech.* **12**, 1–21 (2019).
40. Zhang, L. et al. Sources and processes affecting fine particulate matter pollution over North China: an adjoint analysis of the Beijing APEC Period. *Environ. Sci. Technol.* **50**, 8731–8740 (2016).
41. Tripathi, J., Singh, A. K., Dey, C. & Mukherjee, S. Spatial variation of tropospheric NO_2 concentration during first wave COVID-19 induced lockdown estimated from Sentinel-5 Precursor. Preprint at *Research Square* https://doi.org/10.21203/rs.3.rs-2789162/v1 (2021).
42. Levy, R. & Hsu, C. *MODIS Atmosphere L2 Aerosol Product. NASA MODIS Adaptive Processing System* (Goddard Space Flight Center, 2015).
43. Joanna, J. *GEOS-5 FP-IT Assimilation Geo-colocated to OMI/Aura UV-2 1-Orbit L2 Support Swath 13x24km V3* (NASA Goddard Space Flight Center, 2018).

Acknowledgements

We thank Y. Li and R. Xu for information of the TP, and D. Wu for discussion of nitrogen emission mechanisms. Funding: The Second Tibetan Plateau Scientific Expedition and Research Program grant no. 2019QZKK0604; The National Natural Science Foundation of China grant no. 42075175.

Author contributions

J.L. conceived the research. J.L. and H.K. designed the research. H.K. performed the research. C.L., L.S., X.L., K.Y., H.S. and W.X. commented on the microbial mechanism. Y.Z. helped interpret satellite NO_2 data. C.X. helped interpret the TP environment. H.K. and J.L. analysed the results and wrote the paper with comments from X.L., K.Y. and W.X.

Competing interests

The authors declare no competing interests.

Additional information

Extended data is available for this paper at https://doi.org/10.1038/s41561-023-01200-8.

Supplementary information The online version contains supplementary material available at https://doi.org/10.1038/s41561-023-01200-8.

Correspondence and requests for materials should be addressed to Jintai Lin.

Peer review information *Nature Geoscience* thanks David Fowler, Pertti Martikainen and the other, anonymous, reviewer(s) for their contribution to the peer review of this work. Primary handling editor: Xujia Jiang, in collaboration with the *Nature Geoscience* team.

https://doi.org/10.1038/s41561-023-01200-8

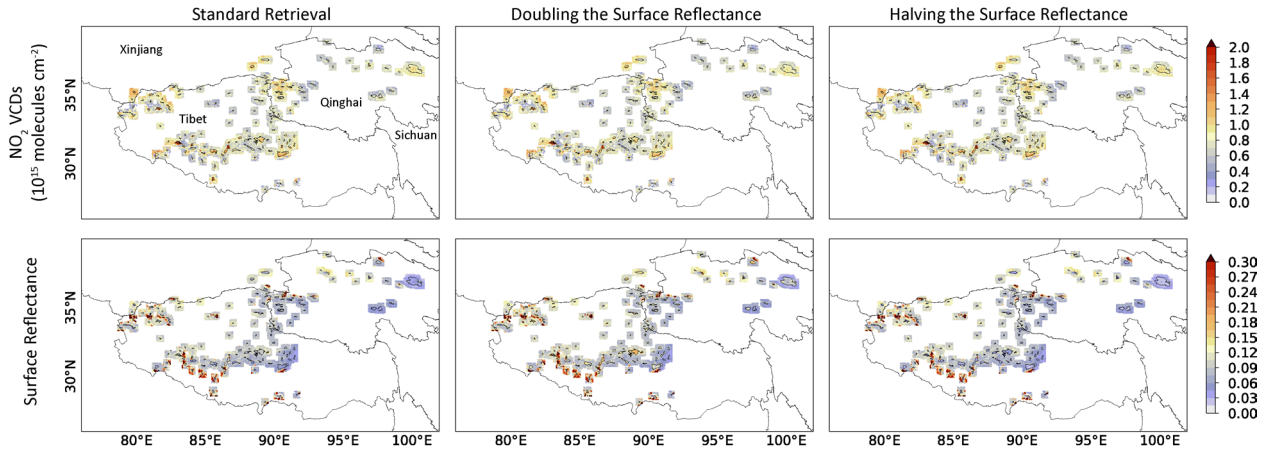

Extended Data Fig. 1 | Sensitivity test of NO_2 VCD retrieval for July 2019. Left column: standard retrieval. Middle column: retrieval by doubling the surface reflectance. Right column: retrieval by halving the surface reflectance.

https://doi.org/10.1038/s41561-023-01200-8

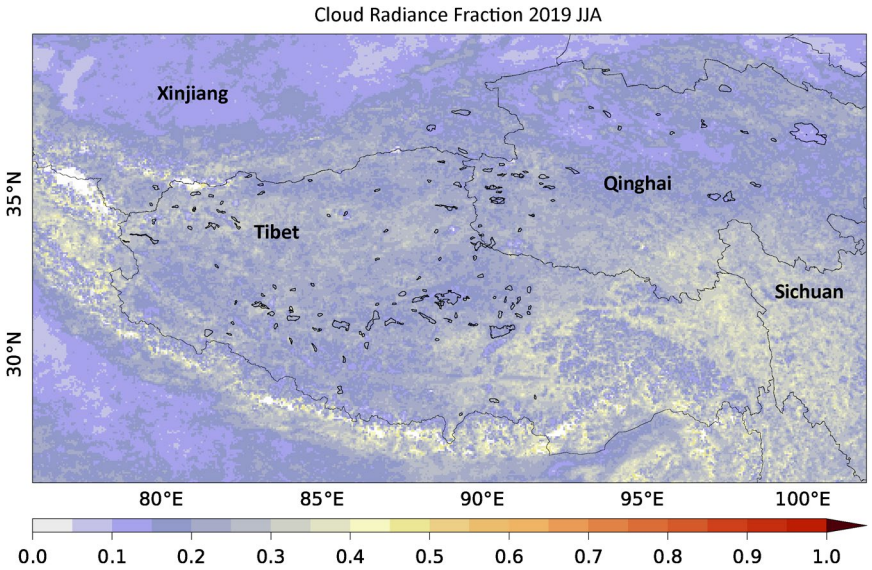

Extended Data Fig. 2 | Distribution of cloud radiance fraction in summer 2019. The 135 lakes studied here are shown with black boundaries and other lakes are shown with blue boundaries. The cloud data are from ref. 1.

https://doi.org/10.1038/s41561-023-01200-8

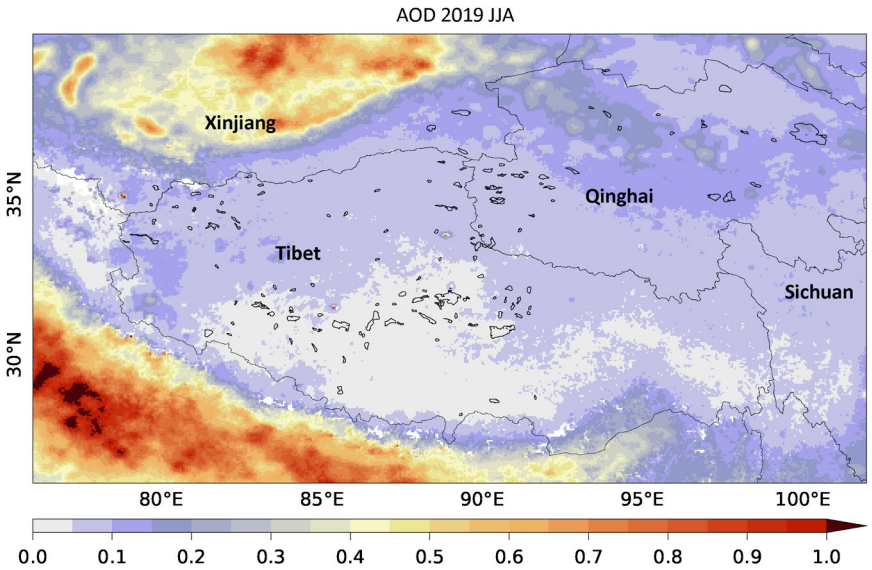

Extended Data Fig. 3 | Distribution of AOD in summer 2019. Data are taken from the MODIS Atmosphere L2 Aerosol Product (ref. 2, MYD04 Collection 6.1, last access: 12/03/2019).